

*Article*

# Effects of In-bed Stoichiometric and Flue Gas Recirculation on Combustion and Environmental Performances of a Swirling Fluidized-bed Combustor

Poramet Arromdee and Kasama Sirisomboon \*

Laboratory of Advance Combustion Technology and Energy Systems, Department of Mechanical Engineering, Faculty of Engineering and Industrial Technology, Silpakorn University, Nakhon Pathom, 73000, Thailand

\*E-mail: sirisomboon\_k@su.ac.th (Corresponding author)

**Abstract.** This work studied the firing of ground nut/peanut shells in a twin-cyclonic fluidized-bed combustor at the maximum combustor loading ( $\sim 22.5$  kg/h) in the flue gas recirculation (FGR) mode. During the experimental tests, excess air (EA) was fixed at about 60%, while the in-bed stoichiometric ratio ( $S_b$ ) and FGR ranged from 1.0-1.2 and from 10-25%, respectively. The experimental results showed that nitrogen oxide ( $NO_x$ ) emissions significantly decreased when FGR increased; however, the opposite tendency was found for carbon monoxide (CO) emission. Meanwhile, FGR showed strong effects on both combustion and emission performances, the impacts of  $S_b$  were quite low. The FGR of  $\sim 10$ -18% and  $S_b$  from 1.0-1.2 appear to be optimum operating conditions for firing ground nut/peanut shells to ensure the lowering of major emissions under the limitations of Thailand's emission standards, with high combustor efficiency at 99%.

**Keywords:** Combustion efficiency;  $NO_x$  reduction, fluidized-bed combustion.

**ENGINEERING JOURNAL** Volume 25 Issue 2

Received 7 February 2020

Accepted 25 November 2020

Published 28 February 2021

Online at <https://engj.org/>

DOI:10.4186/ej.2021.25.2.207

*This article is based on the presentation at the International Conference on Engineering and Industrial Technology (ICEIT 2020) in Chonburi, Thailand, 11th-13th September 2020.*

## 1. Introduction

Among the agricultural residues and organic waste from manufacturing processes, peanut shells are one of the most attractive biomass fuels due to their high calorific values (about 18.5 MJ/kg) [1]; they are also abundant and cheap. In 2017, the production of ground nuts/peanuts (with shells) worldwide was about 47 million tons, with most of the world's production (~62.5%) cultivated in Asia [2]. In Thailand, peanut shells are commonly used as fertilizer. However, in accordance with Thailand's 20-year energy efficiency development plan, peanut shells have recently been used as fuel after the promotion of renewable energy in the Thai government's campaign.

As proven by numerous experimental studies on combustion and emission behaviors in a fluidized-bed combustor (FBC), this technology is recognized as effective for the conversion of biomass to energy as it is environmentally friendly (low NO<sub>x</sub> emissions) with high combustion efficiency [3-7]. However, in the case of firing biomass fuels rich in alkaline metals (potassium, phosphorus, chlorine, and sodium), this combustion technique experiences severe problems due to agglomeration of the bed material and fouling, as well as slagging on the heat transfer surface. In some studies, problems related to the melting of complex eutectic salts on the bed material has been effectively addressed by using alternative bed materials such as alumina sand, dolomite, or limestone [6, 8, 9].

Research studies on firing peanut shells in the FBC have been conducted in fluidized-bed combustion systems by Arromdee and Kuprianov [6], Duan et al. [10], and Duan et al. [11]. Arromdee and Kuprianov studied the firing of shredded peanut shells in a cone-shaped bubbling FBC using alumina as the bed material to avoid the bed agglomeration problem and to increase the catalytic reactions of NO<sub>x</sub> decomposition. During the tests, the used bed material was accumulated at 10 hours, 20 hours, and 30 hours of combustion to analyze the ash composition and size distribution. As indicated in the analysis, none of the particle sampling showed any significant effect of the time scale. However, the number of fine particles (those <300 μm) slightly increased due to collisions, breakage, and attrition of the bed material particles. After 30 hours of use, the alumina sand consisted mainly of K<sub>2</sub>O–Al<sub>2</sub>O<sub>3</sub>–SiO<sub>2</sub> systems (eutectics) which ensured the relatively high melting point (1500-1600°C).

Duan et al. [10] studied the effects of secondary air injection on pollutant emissions in a vortexing fluidized-bed combustor (FBC). In the experimental tests, the secondary gas flow rate was varied from 1.56-2 Nm<sup>3</sup>/min for excess oxygen at 40-55%, with the temperature, pollutant emissions (CO and NO<sub>x</sub>), along with the combustor examined. At this range of operating conditions with the controlling bed temperature below

850°C, CO and NO<sub>x</sub> emissions were found to meet the emission standards of Taiwan's Environmental Protection Administration and the agglomeration of bed material did not occur.

Based on experimental investigations by researchers in fluidized-bed combustion systems, many NO<sub>x</sub> controlling measures have been introduced for biomass fuels. These include the following: co-firing [5], in which the different types of fuels are blended before delivery to the combustor (when a good selection of biomass with an appropriate fuel proportion is made, the NO<sub>x</sub> emission can be mitigated while maintaining high combustion performance); air staging [3], in which the combustion air is separated into primary and secondary flow paths (the appropriate proportion of air is split, corresponding to suitable combustion conditions for NO<sub>x</sub> reduction which normally occurs in the primary combustion zone); fuel staging [11], in which the fuel is unevenly distributed between different combustion zones (the combustion temperature of the primary combustion zone is reduced which reduces NO<sub>x</sub> concentration); and flue gas recirculation (FGR), which seems to be one of the effective techniques for mitigating NO<sub>x</sub> emissions from fuels high in nitrogen [12-16]. In the FGR technique, the flue gas from the stack at 15-20% is supplied back to the combustor with the aim of lowering the temperature of the main combustion zone. This leads to retarding the NO<sub>x</sub> formation through lower oxygen content and higher CO<sub>2</sub> content and is shown to be an effective way for controlling NO<sub>x</sub> emissions.

Duan et al. [12] studied the effects on fuel characteristics when firing crushed and pelletized peanut shells in a wide range of operating conditions in the same combustor as [10] with the aim of investigating the FGR effects. In their study, the flue gas was sucked from the stack and cooled down during the gas cleaning processes to 40-50°C. It was then injected back into the combustor through the wind box with the primary air. In the combustion tests, the primary gas (primary air and FGR) was supplied through a perforated distributor, while the mixture of air and pure nitrogen gas was supplied as the secondary gas through four equally spaced nozzles at a height of 2.05 m above the air distributor. Prior to the tangential injection into the combustor, it was preheated to 200°C. In this process for firing crushed peanut shells, the temperature in the bottom part of the combustor increased with an increase in the in-bed stoichiometric ratio ( $S_b$ ) at a range of 80-110%, while it showed an inverse trend at the freeboard and outlet of the combustor. With the higher  $S_b$  (from 80-110%), the combustion fraction of crushed peanut shells in the bed region gradually increased from about 33-38%, while it slightly decreased in the freeboard from about 67-62%. The CO and NO emissions were also significantly affected by the in-bed stoichiometric ratio ( $S_b$ ). The CO emission increased with the in-bed stoichiometric oxygen ratio, while NO emission showed an inverse trend.

Table 1. Proximate and ultimate analyses of ground nut/peanut shells used in experimental tests.

Ultimate analysis basis (wt. %, as-received basis)					Proximate analysis basis (wt. %, as-received basis)				Lower heating value (MJ/kg)
C	H	O	N	S	W	A	VM	FC	
48.10	5.48	30.04	1.30	0.08	9.3	5.7	65.4	19.6	18,500

The comparative study of the different combustion modes, namely, direct combustion, air-staged combustion, and FGR and their effects on NO emissions was carried out in the same combustor as the work of Duan et al. [10], Chyang et al. [4], and Fang et al. [16]. The experimental results showed that the combustion modes significantly affected both combustion and emission characteristics. The air-staged and FGR combustion could improve emission performance, especially for nitrous oxide (NO). In comparison with direct combustion, FGR could achieve a significant reduction in NO emissions by up to 30%, whereas only 15% reduction was found in air-staged combustion. However, the FGR ratio should be in the appropriate range, with NO emissions found to increase when burning pelletized *Camellia oleifera* shells from 140-180 ppm as the FGR ratio increased from 42-69%.

In the current study, the experimental work aimed to observe the effects of operating conditions (in-bed stoichiometric ratio [ $S_b$ ] and flue gas recirculation [FGR]) on the combustion characteristics and emission performance of a twin-cyclonic swirling fluidized-bed combustor (TS-FBC), firing with ground nut/peanut shells (GPS). The combustion characteristics of the combustor (temperature and  $O_2$  concentration) and the major emissions (CO and NO concentrations) were investigated along the combustor, as well as at the stack. Heat losses owing to incomplete combustion and unburned carbon in fly ash, as well as combustion efficiency, were also discussed.

## 2. Materials and Methods

### 2.1. Experimental Test Facility

Figure 1 shows the components of the experimental set-up included the twin-cyclonic swirling fluidized-bed combustor (TS-FBC) equipped with an annular spiral air distributor, a start-up burner, a cyclone, a fuel screw feeder, heat exchanger, blowers, and an induced draft (ID) fan.

The combustor consisted of twin-cyclonic chambers with the same geometrical dimensions, with each chamber comprising: i) a  $40^\circ$  cone angle conical module (inner diameter of 0.25 m at the bottom and 0.7 m inner diameter at the top, and 1 m in height); and ii) a cylindrical module (0.7 m inner diameter and 0.5 m in height). Both chambers were connected with a 0.25 m inner diameter pipe called the “connecting pipe”. The combustor was fabricated from 7 mm-thick steel metal sheets, and was completely insulated with 100 mm-thick refractory cement to avoid convection and radiation heat losses. The lower chamber

was designed for burning biomass fuel, whereas the upper chamber was designed to ensure complete combustion of the fuel in the freeboard region.

Three sets of air/gas supply systems were assembled for this combustor; primary air, secondary air, and flue gas recirculation (FGR). The primary air was supplied via an annular spiral air distributor to induce swirling fluidization of the gas-solid bed by a 10 hp blower, with the air distributor having 11 blades at  $14^\circ$  angle to the horizontal and a swirl number of 2.76. The secondary air was tangentially injected to the top of the combustor, with two 10 cm-diameter pipes installed in opposite sides of the conical module of the upper chamber 1.6 m above the air distributor ( $Z = 1.6$  m) to control the total excess air (EA) at the specified value. The flue gas was withdrawn from the stack by the 7.5 hp ID fan and cooled to about 50-100°C by a cross-flow heat exchanger. It was then tangentially supplied back to the combustor at a level 0.5 m above the primary air supply system by two 10 cm-diameter pipes installed in opposite sides of the conical module of the lower chamber. The static bed height was fixed at 30 cm above the air distributor for all test runs. During the swirling fluidization mode, the bed material expanded to about 1.5-2 times the static bed height; therefore, it was planned that flue gas recirculation would supply the bed expansion area.

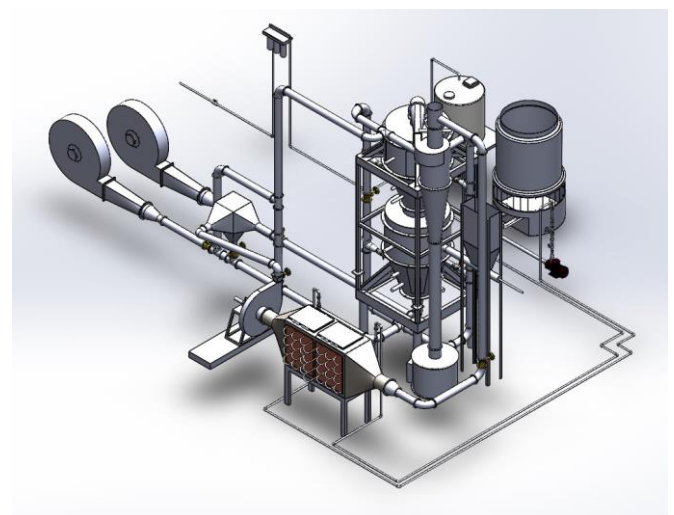


Fig. 1. Schematic diagram of a twin-cyclonic swirling fluidized-bed combustor (TS-FBC).

### 2.2. Fuel and Bed Material

The size of the ground nut/peanut shells (GPS) used in this study ranged from very fine (0-850  $\mu\text{m}$  for 27.8%)

to moderately coarse (1,700-3,500  $\mu\text{m}$  for 35.4% and  $>3,500 \mu\text{m}$  for 36.8%). The average solid bulk density was in the range of 198.74  $\text{kg}/\text{m}^3$ . Table 1 presents the proximate and ultimate analysis as well as the lower heating value calculated from fuel compositions on an as-received basis.

The bed material used in this experiment was silica sand ranging in size from 300–500  $\mu\text{m}$  with a solid density

of 1,700  $\text{kg}/\text{m}^3$ . The static bed height was fixed at 30 cm above the air distributor for all test runs and periodically changed after about 30 hours of usage.

To avoid agglomeration problems with the bed material associated with high temperature during the experimental test runs, the bed temperature was monitored and kept below 950°C.

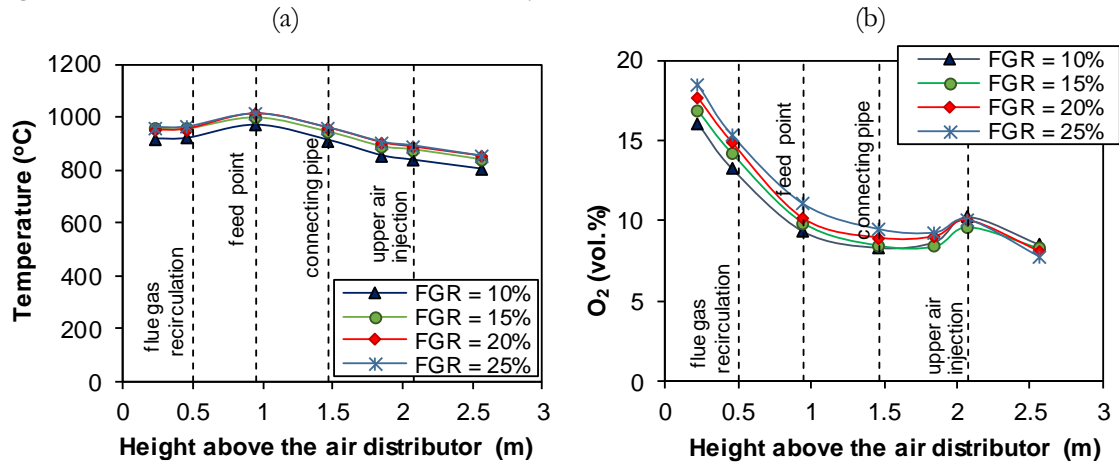


Fig. 2. Effects of FGR on (a) axial temperature and axial and (b) O<sub>2</sub> concentration profiles for firing ground nut/peanut shells at EA ~ 60% and  $S_b = 1.2$ .

### 2.3. Experimental Planning

The experimental tests were conducted to examine the effects of  $S_b$  and FGR on combustion characteristics, major emissions, and efficiency performance of the combustor. The ground nut/peanut shells (GPS) were burned at the fuel feed rate (FR) of 22.5  $\text{kg}/\text{h}$ , the excess air (EA) was fixed at about 60%, and  $S_b$  and FGR were varied in the range of 1.0-1.2 and 10-25% of the primary air flow rate, respectively.

The actual volume of air flow rates for firing ground nut/peanut shells (GPS) at the specified  $S_b$  was calculated based on the theoretical volume of air flow rate at the stoichiometric condition. The flow was then distributed at the identified values to the three air/gas supply systems; primary air, FGR, and secondary air injections. At the same values for  $S_b$  and excess air (EA), the primary air flow rate was fixed at the same specified value. The FGR was varied to determine the effects of this parameter on combustion performance, while the flow rate of secondary air was supplied to the upper combustor chamber with the aim of adjusting the total excess air (EA).

The in-bed stoichiometric ratio ( $S_b$ ) is defined in Eq. (1) as follows:

$$S_b = \frac{\text{Volume of air flowrate in bed region}}{\text{Volume of air flowrate at stoichiometric condition}} \quad (1)$$

where the theoretical volume of air flow rate at the stoichiometric condition ( $V^0$ ,  $\text{m}^3/\text{kg-fuel}$ ) can be calculated from Eq. (2) as follows:

$$V^0 = 0.08899(C^f + 0.375S^f) + 0.265H^f - 0.0333O^f \quad (2)$$

where  $C^f$ ,  $S^f$ ,  $H^f$ , and  $O^f$  are carbon, sulfur, hydrogen, and oxygen contents (%) in fuel on an as-received basis.

The excess air ratio ( $\alpha$ ) for each trial is calculated by Eq. (3) as follows:

$$\alpha = \frac{21}{21 - O_2 - 0.5CO} \quad (3)$$

with O<sub>2</sub> and CO concentrations measured in the flue gas at the stack outlet.

The temperature was measured with seven stationary Chromel-Alumel thermocouples (of type K) along the combustor height at 0.23, 0.46, 0.95, 1.47, 1.85, 2.08, and 2.57 m above the air distributor. The gas concentration was analyzed along the axial direction of the combustor, including the emission gas on the stack. A “Testo-350” gas analyzer (Testo, Germany) was used to measure the gas concentrations, with measurement accuracies  $\pm 0.5\%$  for the temperature;  $\pm 0.2 \text{ vol.}\%$  for O<sub>2</sub>;  $\pm 5\%$  for CO and  $C_xH_y$  ranging from 200-2,000 ppm;  $\pm 10\%$  for CO and  $C_xH_y$  higher than 2,000 ppm; and  $\pm 5\%$  for nitrous oxide (NO).

In the current study, the combustion efficiency ( $\eta_c$ ) was calculated using the heat loss method comprising two major losses: i) heat loss due to non-combustible carbon ( $q_{uc}$ , %); and ii) heat loss due to incomplete combustion of CO ( $q_{ic}$ , %). The  $\eta_c$  was calculated by Eq. (4) as follows:

$$\eta_c = 100 - (q_{uc} + q_{ic}) \quad (4)$$

where  $q_{uc}$  is heat loss of non-combustible carbon (%) and  $q_{ic}$  is heat loss of incomplete combustion (%).

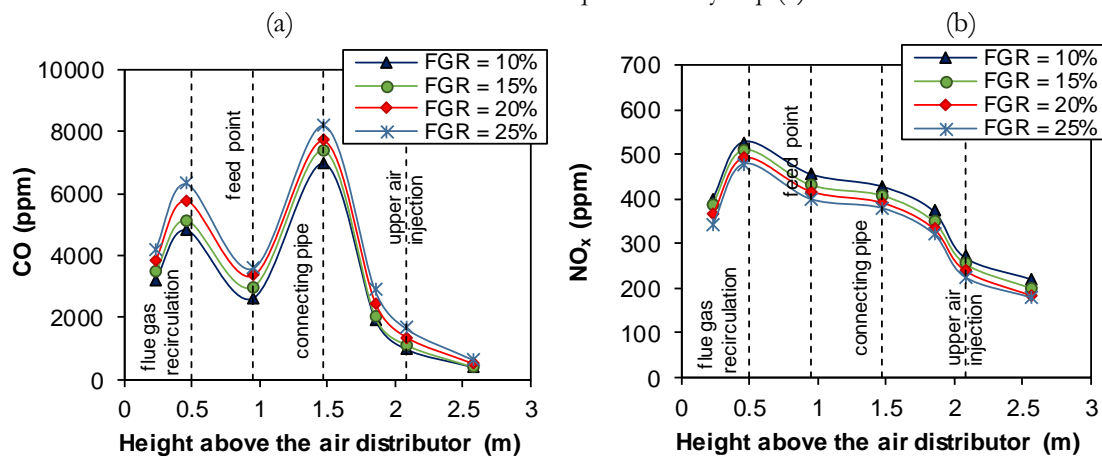


Fig. 3. Effects of FGR on (a) CO and (b) NO<sub>x</sub> concentration profiles for firing ground nut/peanut shells at EA = 60% and  $S_b = 1.2$ ).

$$q_{uc} = \frac{32886}{LHV} \left( \frac{C_{fa}}{100 - C_{fa}} \right) A \quad (5)$$

where LHV is fuel low heating value (kJ/kg);  $C_{fa}$  is unburned carbon in fly ash carried over from the combustor (wt. %); and A is ash composition in fuel on a proximate analysis basis (wt. %).

Heat loss of incomplete combustion ( $q_{ic}$ ) is quantified as the percentage of LHV based on the CO from the combustor (both in ppm, on a dry gas basis and at 6% O<sub>2</sub>) by the following equation:

$$q_{ic} = (126.4CO)_{@6\%O_2} \times 10^{-4} V_{dg@6\%O_2} \frac{(100 - q_{uc})}{LHV} \quad (6)$$

where  $CO_{@6\%O_2}$  is carbon monoxide on a dry gas basis at 6% O<sub>2</sub> and  $V_{dg@6\%O_2}$  is the volume of dry flue gas at 6% O<sub>2</sub>.

### 3. Results and Discussion

#### 3.1. Effects of FGR on Axial Temperature and on O<sub>2</sub> Concentration Profiles

Figure 2 shows the axial temperature and O<sub>2</sub> concentration profiles in the TS-FBC for firing ground nut/peanut shells (GPS); EA is about 60% and  $S_b = 1.2$  for the FGR at 10-25%. As can be seen in Fig. 2(a), the FGR presented slightly significant effects on the axial temperature profiles: the peaks of the temperature were found near the level of the fuel feeding point (0.95 m above the air distributor) for all test runs. The axial temperatures showed a gradual decrease along the height of the combustor which can be explained by the heat loss across the combustor walls. The temperatures at each location along the combustor slightly increased with the increasing FGR, with this likely to be due to the higher

Heat loss of non-combustible carbon ( $q_{uc}$ ) is the incomplete combustion of carbon in fly ash. It was quantified by Eq. (5) as follows:

amount of FGR carrying more heat to the combustor. This trend also occurred in the experimental study conducted by Chyang et al. [4], in which corn cobs were fired in the vortexing FBC, however, with the FGR having less impact.

The O<sub>2</sub> concentration profiles for firing ground nut/peanut shells (GPS) under different levels of FGR are shown in Fig. 2(b). As can be seen, the O<sub>2</sub> concentration significantly decreased in the lower section of the combustor. However, it slightly increased near to the level of secondary air injection and decreased again at the above level. Accounting for the O<sub>2</sub> tendency, together with the temperature profiles, this indicated that the vigorous combustion of coarse fuel particles and volatile matter mainly occurred above the bed and below the fuel feeding point in the lower combustor chamber (at  $Z = 0-0.95$  m above the air distributor). The combustion of fine fuel particles and some remaining volatile matter seemed to occur in the upper combustor chamber.

The results showed that, with rising FGR, the O<sub>2</sub> concentration increased in the lower combustor chamber. However, the opposite occurred for the level above the secondary air injection, which can be explained by the splitting values of the different sources of air supply. With this firing technique, for the fixed  $S_b$  and EA at the higher value of FGR, less O<sub>2</sub> was supplied through the secondary air injection.

#### 3.2. Effects of FGR on Axial CO and NO<sub>x</sub> Concentration Profiles

Figure 3 shows the axial CO and NO<sub>x</sub> concentration profiles in the TS-FBC at the same operating conditions as Fig. 2. As can be seen in Fig. 3(a), the axial CO concentration profiles were found to have two peaks, that is, at: i) the levels of flue gas recirculation, and ii) the connecting pipe between the lower and upper reactors (at  $Z = 1.47$  m) for all operating conditions. The first peak

can be explained by the fuel devolatilization that normally occurred near the fuel feeding level (at  $Z = 0.95$  m), together with the CO from the flue gas recirculation (FGR). After the CO was continuously oxidized by primary air and  $O_2$  from FGR below the feeding point, its level noticeably increased at the connecting pipe, and

sharply decreased at the top of the combustor. While flowing through the connecting pipe, the products of combustion in the combustor were compressed into a smaller volume; therefore, the concentration of gases significantly increased as can be seen in the second peak in Fig. 3(a).

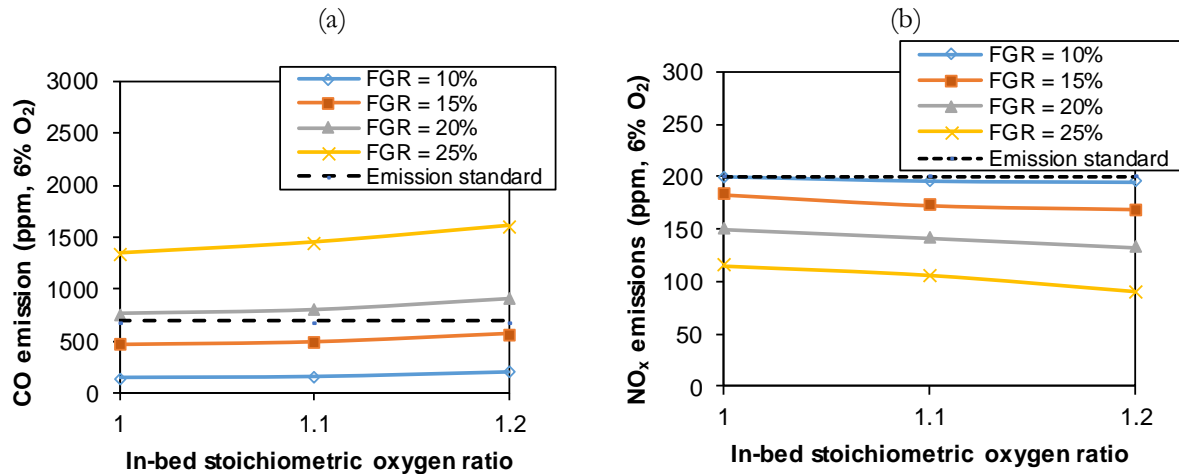


Fig. 4. Effects of in-bed stoichiometric oxygen ratio and FGR on (a) CO and (b)  $NO_x$  emissions for firing ground nut/peanut shells at EA of about 60%.

With FGR increasing at the same EA and  $S_b$ , the CO concentration increased at all locations along the height of the combustor, especially at the FGR level, mainly due to the higher CO from the flue gas, although the effect of FGR was quite trivial at the top of combustor.

Within this range of operating conditions (the bed temperature controlled under  $950^\circ C$ ),  $NO_x$  in the flue gas mainly occurred from the Fuel-N mechanism via the homogeneous oxidation of the Volatile-N species, such as HCN and  $NH_3$  [9, 11]. Unlike the axial CO concentration profiles, the axial  $NO_x$  concentration profiles were found to have only one maximum value near the level of FGR (and below the fuel feeding point,  $Z = 0.5$  m). The  $NO_x$  concentration then continuously decreased along the height of the reactor. As can be seen in Fig. 3(a) and Fig. 3(b), the  $NO_x$  concentration profiles show an inverse tendency for the CO concentration with the increasing FGR, which can be explained by the decomposed reactions of NO with CO via heterogeneous reactions. In a homogeneous reaction, the NO reduction mainly occurs in the flame by radicals such as  $CH_i$  ( $CH/CH_2$ ),  $NH_i$  ( $NH/NH_2$ ), and HCCO [14, 17], while it is also catalytically accelerated by CO, with char and ash as catalysts in heterogeneous reactions [17-19].

### 3.3. Effects of $S_b$ and FGR on Major Emissions

Figure 4 shows the effects of the in-bed stoichiometric oxygen ratio and FGR on (a) CO and (b)  $NO_x$  emissions for firing ground nut/peanut shells (GPS) at EA of about 60%. The results showed that FGR had a significant effect on both emissions, while the effects of  $S_b$  were quite weak. With increasing FGR at a fixed  $S_b$ , CO

emissions were found to increase, while the opposite was true for  $NO$  emissions that were found to decrease.

The effects of FGR on  $NO_x$  emissions in the current study are quite inconsistent with the results of Li and Chyang [20]. However, the different experimental methodology and different combustion systems may have had an effect on the experimental results. In their study, the FGR percentage increased with a decreasing  $S_b$ , while, in our experiment, the change in  $S_b$  does not affect the FGR percentage. In their study,  $NO_x$  emissions for firing coal, corn cobs, and rice husks increased with an increasing FGR, with their explanation being that the optimal range of stoichiometry in the bed for each fuel is quite different. The increasing FGR may not be able to reduce  $NO_x$  emissions during the combustion of all types of fuel.

As revealed in the experimental results in our study on firing ground nut/peanut shells (GPS) in the TS-FBC, to satisfy Thai emission standards, the FGR should be limited to the range of 10-15% for the  $S_b$ , with the range of 1-1.2 for EA of about 60%.

### 3.4. Effects of $S_b$ and FGR on Combustion Efficiency

Table 2 shows the combustion efficiency and major emissions at the stack outlet. As can be seen, the combustion efficiency shows slightly significant effects for  $S_b$  and flue gas recirculation (FGR). Both unburned carbon ( $q_{uc}$ ) and incomplete combustion ( $q_{ic}$ ) from these experimental tests were quite small, in the range 0.4-0.7% and 0.1-0.7%, respectively, so combustor efficiency can be achieved at a value of about 99%.

Table 2. Emissions and combustion efficiency of a TS-FBC for firing ground nut/peanut shells with FGR at various in-bed stoichiometric ratios ( $S_b$ ) for EA of about 60%.

EA (%)	$S_b$	FGR (%)	$C_{fa}$ (%)	$q_{uc}$ (%)	$q_{ic}$ (%)	Combustion efficiency (%)
60.1	1.0	10	5.90	0.63	0.07	99.30
58.9		15	6.77	0.74	0.21	99.06
60.7		20	6.12	0.66	0.34	99.00
59.3		25	3.47	0.36	0.60	99.04
59.3	1.1	10	5.74	0.62	0.07	99.31
60.4		15	6.84	0.74	0.22	99.04
60.7		20	6.11	0.66	0.36	98.98
59.1		25	3.54	0.37	0.65	98.98
62.4	1.2	10	5.56	0.60	0.09	99.31
59		15	6.78	0.74	0.25	99.01
61.3		20	6.26	0.68	0.41	98.92
60.8		25	3.52	0.37	0.72	98.91

#### 4. Conclusions

In the current study, emission characteristics including axial temperature,  $O_2$ , CO, and NO concentration profiles as well as combustion efficiency were investigated in a conical fluidized-bed combustor with flue gas recirculation (FGR). The results can be summarized as follows:

- Flue gas recirculation (FGR) shows noticeable effects on  $NO_x$  and CO emissions, while the effects of  $S_b$  are quite weak.
- Nitrous oxide ( $NO_x$ ) emissions significantly decreased with increasing FGR; however, the opposite tendency was found for CO emissions.
- Optimum operation for firing ground nut/peanut shells (GPS) seems to be in from ~10-18% for FGR and from 1.0-1.2 for  $S_b$  at EA of about 60%.
- In our range of tests, combustion efficiency was found to be high at a value of about 99%.

#### Acknowledgements

The authors wish to acknowledge Mr Tananon Srisamran for his helpful on the experimental tests, as well as their gratitude for financial support from Silpakorn University Research, Innovation and Creative Fund, and Department of Mechanical Engineering, Faculty of Engineering and Industrial Technology, Silpakorn University.

#### References

[1] M. A. Perea-Moreno, F. Manzano-Agugliaro, Q. Hernandez-Escobedo, and A. J. Perea-Moreno, "Peanut Shell for Energy: Properties and Its

- Potential to Respect the Environment," *Sustainability*, vol. 10, pp. 3254-3272, 2018.
- [2] FAO, "Production quantities of Groundnuts, with shell by country 2017," FAO Departments and Offices, 2017. [Online]. Available: <http://www.fao.org> (accessed 15 October 2019).
- [3] K. Sirisomboon and P. Charernporn, "Effects of air staging on emission characteristics in a conical fluidized-bed combustor firing with sunflower shells," *J Energy Inst*, vol. 90, pp. 316-323, 2017.
- [4] C. S. Chyang, F. Duan, S. M. Lin, and J. Tso, "A study on fluidized bed combustion characteristics of corncob in three different combustion modes," *Bioresour Technol*, vol. 116, pp. 184-189, 2012.
- [5] S. Chakritthakul and V. I. Kuprianov, "Co-firing of eucalyptus bark and rubberwood sawdust in a swirling fluidized-bed combustor using an axial flow swirler," *Bioresour Technol*, vol. 102, pp. 8268-8278, 2011.
- [6] P. Ninduangdee and V. I. Kuprianov, "Combustion of oil palm shells in a fluidized-bed combustor using dolomite as the bed material to prevent bed agglomeration," *Energy Procedia*, vol. 52, pp. 399-409, 2014.
- [7] P. Arromdee and V.I. Kuprianov, "Experimental study and empirical modeling of CO and NO behaviors in a fluidized-bed combustor firing pelletized biomass fuels," *Biomass Convers Bior*, to be published.
- [8] P. Ninduangdee and V. I. Kuprianov, "Study on burning oil palm kernel shell in a conical fluidized-bed combustor using alumina as the bed material," *J Taiwan Inst Chem E*, vol. 44, pp. 1045-1053, 2013.
- [9] P. Arromdee and V. I. Kuprianov, "Combustion of peanut shells in a cone-shaped bubbling fluidized-bed combustor using alumina as the bed material," *Appl. Energy*, vol. 97, pp. 470-482, 2012.
- [10] F. Duan, C. S. Chyang, Y. J. Wang, and J. Tso, "Effect of secondary gas injection on the peanut shell combustion and its pollutant emissions in a vortexing fluidized bed combustor," *Bioresour Technol* vol. 154, pp. 201-208, 2014.
- [11] K. Sirisomboon and V. I. Kuprianov, "Effects of fuel staging on the NO emission reduction during biomass-biomass co-combustion in a fluidized-bed combustor," *Energy Fuels*, vol. 31, pp. 659-671, 2017.
- [12] F. Duan, L. H. Zhang, C. S. Chyang, J. L. Wang, and P. S. Li, "Combustion of crushed and pelletized peanut shells in a pilot-scale fluidized-bed combustor with flue gas recirculation," *Fuel Process Technol*, vol. 128, pp. 28-35, 2014.
- [13] F. Duan, C. S. Chyang, S. M. Lin, and J. Tso, "Experimental study on rice husk combustion in a vortexing fluidized-bed with flue gas recirculation (FGR)," *Bioresour Technol*, vol. 134, pp. 204-211, 2013.
- [14] P. W. Li and C. S. Chyang, "A comprehensive study on  $NO_x$  emission and fuel nitrogen conversion of solid biomass in bubbling fluidized beds under

- staged combustion.,” *J Energy Inst*, vol. 93, pp. 324-334, 2020.
- [15] M. B. Nordenkampf, “Staged combustion and exhaust gas recirculation in fluidized beds,” in *Handbook of Combustion*. Weinheim: Wiley-VCH Verlag GmbH & Co. KGaA, 2015, ch. 7, vol. 5, pp. 161–179.
- [16] D. D. Fang, L.H. Zhang, F. Duan, C. S. Chyang, and Y. C. Wang, “Combustion and pollutant emissions characteristics of *Camellia oleifera* shells in a vortexing fluidized-bed combustor,” *J Energy Inst*, to be published.
- [17] H. Spliethoff, U. Greul, H. Rüdiger, and K. R. G. Hein, “Basic effects on NO<sub>x</sub> emissions in air staging and reburning at a bench-scale test facility,” *Fuel*, vol. 75 pp. 560-564, 1996.
- [18] P. Ninduangdee and V. I. Kuprianov, “Fluidized bed co-combustion of rice husk pellets and moisturized rice husk: The effects of co-combustion methods on gaseous emissions,” *Biomass Bioenergy*, vol. 112, pp. 73-84, 2018.
- [19] G. Olofsson, W. Wang, Z. Ye, I. Bjerle, and A. Andersson, “Repressing NO<sub>x</sub> and N<sub>2</sub>O emissions in a fluidized bed biomass combustor,” *Energy Fuels*, vol. 16, pp. 915-919, 2002.
- [20] P. W. Li and C. S. Chyang, “A comprehensive study on NO<sub>x</sub> emission and fuel nitrogen conversion of solid biomass in bubbling fluidized beds under staged combustion,” *J Energy Inst*, to be published.



**Poramet Arromdee** was born in Bangkok, Thailand in 1982 .He received his B.Eng in mechanical engineering from Sirindhorn International Institute of Technology (SIIT), Thammasat University, Thailand in 2005, M.Eng Sci in Mechanical Engineering from The University of New South Wales, Australia in 2006, and the Ph.D. in Mechanical Engineering from Sirindhorn International Institute of Technology (SIIT), Thammasat University, Thailand in 2012. He is currently a lecturer at Department of Mechanical Engineering, Faculty of Engineering and Industrial Technology, Silpakorn University. His research interests include energy engineering, biomass fuels, fluidized-bed combustion systems.



**Kasama Sirisomboon** was born in Bangkok, Thailand in 1976. She received the B.Eng in mechanical engineering from Khon Kaen University in 1997, M.Eng in energy technology King Mongkut's University of Thonburi (KMUTT) in 2000 and the Ph.D. degree in mechanical engineering program from Sirindhorn International Institute of Technology (SIIT), Thammasat University, in 2008.

From 1997 to 2003, she was a lecturer at department of mechanical engineering, Ubon Ratchathani University. Since 2008, she has been an Associate Professor with the Mechanical Engineering Department, faculty of Engineering and Industrial Technology, Silpakorn University. She is the author of two books, and more than 16 articles. Her research interests include fluidized-bed biomass combustion and renewable energy. Dr. Kasama was a recipient of the International Conference on Science, Technology and Innovation for Sustainable Well-Being (STISTWB) Best Paper Award in 2018.